Inorg. Chem. **2006**, *45*, 1215–1227

Syntheses and Quadratic Optical Nonlinearities of Ruthenium(II) Complexes with Ethynyl-Connected *N*-Methylpyridinium Electron Acceptors

Benjamin J. Coe,*,† Josephine L. Harries,† Madeleine Helliwell,† Bruce S. Brunschwig,‡ James A. Harris,‡ Inge Asselberghs,§ Sheng-Ting Hung,§ Koen Clays,§ Peter N. Horton,|| and Michael B. Hursthouse||

School of Chemistry, University of Manchester, Oxford Road, Manchester M13 9PL, U.K., Molecular Materials Research Center, Beckman Institute, MC 139-74, California Institute of Technology, 1200 East California Boulevard, Pasadena, California 91125, Department of Chemistry, University of Leuven, Celestijnenlaan 200D, B-3001 Leuven, Belgium, and EPSRC National Crystallography Service, School of Chemistry, University of Southampton, Highfield, Southampton SO17 1BJ, U.K.

Received October 20, 2005

We have prepared a number of new dipolar complexes containing ethynyl or buta-1,3-diynyl units linking electron-rich $\{Ru^{II}(NH_3)_5\}^{2+}$, *trans*-$\{Ru^{II}(NH_3)_4L\}^{+}$ (L = pyridine or *N*-methylimidazole), or *trans*-$\{Ru^{II}Cl(pdma)_2\}^{+}$ [pdma = 1,2-phenylenebis(dimethylarsine)] centers to pyridinium electron acceptors. In acetonitrile solutions at 295 K, the new complexes display unusual blue-shifting of their metal-to-ligand charge-transfer (MLCT) bands as the conjugation is extended, in a fashion similar to that of the corresponding ethenyl systems. Hyper-Rayleigh scattering (HRS) and Stark spectroscopic measurements provide direct and indirect estimates of static first hyperpolarizabilities β_0, and both the linear and nonlinear optical (NLO) properties are temperature- and medium-dependent. Thus, at 77 K in butyronitrile glasses, the MLCT bands display more normal red shifts upon conjugation extension. While the Stark-derived β_0 values generally increase as n (the number of ethynyl units) increases from 0 to 2, the HRS data show maximization at $n = 1$ for two of the ammine series but an increase upon moving from $n = 1$ to 2 for the pdma complexes. Comparisons with the analogous ethenyl chromophores show that the latter generally display larger β_0 values, whether determined via HRS or Stark data, and the inferiority of the ethynyl systems in terms of NLO response is more pronounced when $n = 2$. This differing behavior is attributable primarily to larger increases in the transition dipole moment μ_{12} (and, hence, donor–acceptor π-electronic coupling) on elongation in the ethenyl chromophores.

Introduction

Organic compounds that manifest nonlinear optical (NLO) effects continue to attract considerable interest, primarily because of their potential for uses in optical data processing technologies.[1] Various optoelectronic applications require quadratic (second-order) NLO properties, while cubic (third-order) effects hold promise for exploitation in all-optical devices. Measurements and calculations of first and second hyperpolarizabilities β and γ, which respectively produce quadratic and cubic NLO effects, have shown that a broad array of chromophores can show large molecular responses. Transition metal complexes are a particularly interesting subclass of such compounds because they can add extra

* To whom correspondence should be addressed. E-mail: b.coe@man.ac.uk.
† University of Manchester.
‡ California Institute of Technology.
§ University of Leuven.
|| University of Southampton.

(1) (a) Zyss, J. *Molecular Nonlinear Optics: Materials, Physics and Devices*; Academic Press: Boston, 1994. (b) Bosshard, Ch.; Sutter, K.; Prêtre, Ph.; Hulliger, J.; Flörsheimer, M.; Kaatz, P.; Günter, P. Organic Nonlinear Optical Materials. *Advances in Nonlinear Optics*; Gordon & Breach: Amsterdam, The Netherlands, 1995. (c) *Nonlinear Optics of Organic Molecules and Polymers*; Nalwa, H. S., Miyata, S., Eds.; CRC Press: Boca Raton, FL, 1997. (d) *Nonlinear Optical Properties of Matter: From Molecules to Condensed Phases*; Papadopoulos, M. G., Leszczynski, J., Sadlej, A. J., Eds.; Kluwer: Dordrecht, The Netherlands, 2006.

10.1021/ic051816+ CCC: $33.50
Published on Web 01/11/2006

functionality to the attractive optical properties of organic species.[2] The promise of metal complexes in this field is nicely illustrated by several reports in which metal-based redox is used to switch NLO responses (both quadratic and cubic).[3] Large β coefficients are characteristic of π-conjugated molecules that feature strongly electron-donating (D) and -accepting (A) termini, and such chromophores also display D $\rightarrow$ A intramolecular charge-transfer (ICT) excitations. Experimentally determined β values are hence normally enhanced by resonance, and static first hyperpolarizabilities β_0 must be derived in order to establish molecular structure−activity correlations. Most metal-based NLO chromophores feature electron-rich metal center(s), and their β responses are thus associated with metal-to-ligand charge-transfer (MLCT) transitions.

We have previously described detailed experimental and theoretical investigations into the quadratic NLO behavior of a range of complex species containing ruthenium(II) D groups and pyridinium acceptors.[3a,4] Because the extension of π-conjugated bridges is a common strategy for increasing β responses in organic chromophores,[1] we have prepared and studied a series of complexes containing polyenylpyridyl ligands. Interestingly, this work afforded the unexpected result that the MLCT bands begin to blue-shift with extension beyond a single (*E*)-ethenyl linkage, in marked contrast to the behavior of almost all known purely organic or metal-containing D−A polyenes in which ICT bands red-shift as the chain length increases.[5] Furthermore, the β_0 responses of our complexes show maximization at a (*E*,*E*)-buta-1,3-dienyl linkage, beginning to drop off for $n = 3$ [where n is the number of (*E*)-ethenyl units], while β_0 has been found to increase steadily with n (at least for synthetically accessible chain lengths) in all other systems studied. Given our unusual observations with polyene chromophores, it is clearly of interest to ascertain whether similar behavior is observed in related π-conjugated species, and we have therefore prepared a number of ruthenium(II) ammine complexes of pyridyl ligands bearing pyridinium acceptors connected via ethynyl linkages. Several previous comparative theoretical NLO studies with purely organic ethenyl and ethynyl D−A chromophores have appeared,[6] but the available corresponding experimental data are very limited.[7] These reports generally indicate that ethynyl units provide less effective D−A electronic communication when compared with ethenyl bridges and therefore lead to considerably lower β responses.[6,7] Clearly, the more effective orbital overlap between a sp^2-hybridized CH=CH bond (as opposed to a sp-hybridized C≡C bond) and an aryl ring is an important factor in chromophores with aryl termini. The π orbitals of an ethenyl unit lie closer in energy to those of an aryl ring than do the orbitals of an ethynyl unit in which the smaller internuclear separation causes stabilization of the local highest occupied molecular orbital (HOMO) and destabilization of the local lowest unoccupied molecular orbital

(2) (a) Kanis, D. R.; Ratner, M. A.; Marks, T. J. *Chem. Rev.* **1994**, *94*, 195. (b) Long, N. J. *Angew. Chem., Int. Ed. Engl*. **1995**, *34*, 21. (c) Whittall, I. R.; McDonagh, A. M.; Humphrey, M. G.; Samoc, M. *Adv. Organomet. Chem*. **1998**, *42*, 291. (d) Whittall, I. R.; McDonagh, A. M.; Humphrey, M. G.; Samoc, M. *Adv. Organomet. Chem*. **1998**, *43*, 349. (e) Heck, J.; Dabek, S.; Meyer-Friedrichsen, T.; Wong, H. *Coord. Chem. Rev*. **1999**, *190*−*192*, 1217. (f) Gray, G. M.; Lawson, C. M. In *Optoelectronic Properties of Inorganic Compounds*; Roundhill, D. M., Fackler, J. P., Jr., Eds.; Plenum: New York, 1999; pp 1−27. (g) Shi, S. In *Optoelectronic Properties of Inorganic Compounds*; Roundhill, D. M., Fackler, J. P., Jr., Eds.; Plenum: New York, 1999; pp 55−105. (h) Le Bozec, H.; Renouard, T. *Eur. J. Inorg. Chem*. **2000**, 229. (i) Barlow, S.; Marder, S. R. *Chem. Commun.* **2000**, 1555. (j) Lacroix, P. G. *Eur. J. Inorg. Chem*. **2001**, 339. (k) Di Bella, S. *Chem. Soc. Rev.* **2001**, *30*, 355. (l) Coe, B. J. In *Comprehensive Coordination Chemistry II*; McCleverty J. A., Meyer, T. J., Eds.; Elsevier Pergamon: Oxford, U.K., 2004; Vol. 9, pp 621−687.

(3) (a) Coe, B. J.; Houbrechts, S.; Asselberghs, I.; Persoons, A. *Angew. Chem., Int. Ed.* **1999**, *38*, 366. (b) Weyland, T.; Ledoux, I.; Brasselet, S.; Zyss, J.; Lapinte, C. *Organometallics* **2000**, *19*, 5235. (c) Malaun, M.; Reeves, Z. R.; Paul, R. L.; Jeffery, J. C.; McCleverty, J. A.; Ward, M. D.; Asselberghs, I.; Clays, K.; Persoons, A. *Chem. Commun*. **2001**, 49. (d) Malaun, M.; Kowallick, R.; McDonagh, A. M.; Marcaccio, M.; Paul, R. L.; Asselberghs, I.; Clays, K.; Persoons, A.; Bildstein, B.; Fiorini, C.; Nunzi, J.-M.; Ward, M. D.; McCleverty, J. A. *J. Chem. Soc., Dalton Trans.* **2001**, 3025. (e) Cifuentes, M. P.; Powell, C. E.; Humphrey, M. G.; Heath, G. A.; Samoc, M.; Luther-Davies, B. *J. Phys. Chem. A* **2001**, *105*, 9625. (f) Paul, F.; Costuas, K.; Ledoux, I.; Deveau, S.; Zyss, J.; Halet, J.-F.; Lapinte, C. *Organometallics* **2002**, *21*, 5229. (g) Powell, C. E.; Cifuentes, M. P.; Morrall, J. P.; Stranger, R.; Humphrey, M. G.; Samoc, M.; Luther-Davies, B.; Heath, G. A. *J. Am. Chem. Soc*. **2003**, *125*, 602. (h) Asselberghs, I.; Clays, K.; Persoons, A.; McDonagh, A. M.; Ward, M. D.; McCleverty, J. A. *Chem. Phys. Lett.* **2003**, *368*, 408. (i) Powell, C. E.; Humphrey, M. G.; Cifuentes, M. P.; Morrall, J. P.; Samoc, M.; Luther-Davies, B. *J. Phys. Chem. A* **2003**, *107*, 11264. (j) Sporer, C.; Ratera, I.; Ruiz-Molina, D.; Zhao, Y.; Vidal-Gancedo, J.; Wurst, K.; Jaitner, P.; Clays, K.; Persoons, A.; Rovira, C.; Veciana, J. *Angew. Chem., Int. Ed.* **2004**, *43*, 5266.

(4) For selected recent examples, see: (a) Coe, B. J.; Jones, L. A.; Harris, J. A.; Sanderson, E. E.; Brunschwig, B. S.; Asselberghs, I.; Clays, K.; Persoons, A. *Dalton Trans*. **2003**, 2335. (b) Coe, B. J.; Jones, L. A.; Harris, J. A.; Brunschwig, B. S.; Asselberghs, I.; Clays, K.; Persoons, A. *J. Am. Chem. Soc.* **2003**, *125*, 862. (c) Coe, B. J.; Jones, L. A.; Harris, J. A.; Brunschwig, B. S.; Asselberghs, I.; Clays, K.; Persoons, A.; Garín, J.; Orduna, J. *J. Am. Chem. Soc.* **2004**, *126*, 3880. (d) Coe, B. J.; Harris, J. A.; Jones, L. A.; Brunschwig, B. S.; Song, K.; Clays, K.; Garín, J.; Orduna, J.; Coles, S. J.; Hursthouse, M. B. *J. Am. Chem. Soc.* **2005**, *127*, 4845.

(5) For representative examples, see: (a) Blanchard-Desce, M.; Alain, V.; Bedworth, P. V.; Marder, S. R.; Fort, A.; Runser, C.; Barzoukas, M.; Lebus, S.; Wortmann, R. *Chem.*−*Eur. J.* **1997**, *3*, 1091. (b) Bublitz, G. U.; Ortiz, R.; Runser, C.; Fort, A.; Barzoukas, M.; Marder, S. R.; Boxer, S. G. *J. Am. Chem. Soc.* **1997**, *119*, 2311. (c) Lee, I. S.; Seo, H.; Chung, Y. K. *Organometallics* **1999**, *18*, 1091. (d) Jayaprakash, K. N.; Ray, P. C.; Matsuoka, I.; Bhadbhade, M. M.; Puranik, V. G.; Das, P. K.; Nishihara, H.; Sarkar, A. *Organometallics* **1999**, *18*, 3851. (e) Farrell, T.; Meyer-Friedrichsen, T.; Malessa, M.; Haase, D.; Saak, W.; Asselberghs, I.; Wostyn, K.; Clays, K.; Persoons, A.; Heck, J.; Manning, A. R. *J. Chem. Soc., Dalton Trans*. **2001**, 29. (f) Lawrentz, U.; Grahn, W.; Lukaszuk, K.; Klein, C.; Wortmann, R.; Feldner, A.; Scherer, D. *Chem.*−*Eur. J.* **2002**, *8*, 1573.

(6) (a) Jain, M.; Chandrasekhar, J. *J. Phys. Chem.* **1993**, *97*, 4044. (b) Morley, J. O. *Int. J. Quantum Chem.* **1993**, *46*, 19. (c) Morley, J. O. *J. Phys. Chem.* **1995**, *99*, 10166. (d) Albert, I. D. L.; Morley, J. O.; Pugh, D. *J. Phys. Chem. A* **1997**, *101*, 1763. (e) Jacquemin, D.; Champagne, B.; André, J.-M. *Int. J. Quantum Chem.* **1997**, *65*, 679. (f) Champagne, B.; Kirtman, B. *Chem. Phys.* **1999**, *245*, 213. (g) Lee, J. Y.; Suh, S. B.; Kim, K. S. *J. Chem. Phys.* **2000**, *112*, 344.

(7) Cheng, L.-T.; Tam, W.; Marder, S. R.; Stiegman, A. E.; Rikken, G.; Spangler, C. W. *J. Phys. Chem.* **1991**, *95*, 10643.

(8) (a) Behrens, U.; Brussaard, H.; Hagenau, U.; Heck, J.; Hendrickx, E.; Körnich, J.; van der Linden, J. G. M.; Persoons, A.; Spek, A. L.; Veldman, N.; Voss, B.; Wong, H. *Chem.*−*Eur. J.* **1996**, *2*, 98. (b) Whittall, I. R.; Cifuentes, M. P.; Humphrey, M. G.; Luther-Davies, B.; Samoc, M.; Houbrechts, S.; Persoons, A.; Heath, G. A.; Hockless, D. C. R. *J. Organomet. Chem.* **1997**, *549*, 127. (c) Whittall, I. R.; Cifuentes, M. P.; Humphrey, M. G.; Luther-Davies, B.; Samoc, M.; Houbrechts, S.; Persoons, A.; Heath, G. A.; Bogsanyi, D. *Organometallics* **1997**, *16*, 2631. (d) Wu, I.-Y.; Lin, J. T.; Luo, J.; Li, C.-S.; Tsai, C.; Wen, Y. S.; Hsu, C.-C.; Yeh, F.-F.; Liou, S. *Organometallics* **1998**, *17*, 2188. (e) Hurst, S. K.; Cifuentes, M. P.; Morrall, J. P. L.; Lucas, N. T.; Whittall, I. R.; Humphrey, M. G.; Asselberghs, I.; Persoons, A.; Samoc, M.; Luther-Davies, B.; Willis, A. C. *Organometallics* **2001**, *20*, 4664.

(LUMO). A small number of studies involving related transition metal complexes with single ethenyl or ethynyl bridging units have also been reported, and these all show the same superiority of a (*E*)-CH═CH with respect to a C≡C linkage in terms of β enhancement.[8]

Experimental Section

Materials and Procedures. The compound 1,2-phenylenebis(dimethylarsine) (pdma) was obtained from Dr. G. Reid, University of Southampton, Southampton, U.K. The compounds $[Ru^{II}(NH_3)_5(H_2O)][PF_6]_2$,[9] *trans*-$[Ru^{II}Cl(NH_3)_4(SO_2)]Cl$,[9] *trans*-$[Ru^{III}(SO_4)(NH_3)_4(py)]Cl$ (py = pyridine),[9] *trans*-$[Ru^{II}Cl(pdma)_2(NO)][PF_6]_2$,[10] bis(4-pyridyl)acetylene (bpa),[11] 1,4-bis(4-pyridyl)buta-1,3-diyne (bpbd),[12] and 1,4-bis(4-pyridylethynyl)benzene (bpeb)[13] were prepared according to published procedures. All other reagents were obtained commercially and used as supplied. All reactions were performed under an argon atmosphere. Products were dried at room temperature in a vacuum desiccator ($CaSO_4$) for ca. 24 h prior to characterization.

General Physical Measurements. ^{1}H NMR spectra were recorded on a Varian Gemini 200 or a Varian XL-300 spectrometer, and all shifts are referenced to tetramethylsilane. The fine splitting of pyridyl or phenyl ring AA′BB′ patterns is ignored, and the signals are reported as simple doublets, with *J* values referring to the two most intense peaks. Elemental analyses were performed by the Microanalytical Laboratory, University of Manchester, Manchester, U.K., and UV−visible spectra were obtained by using a Hewlett-Packard 8452A diode array spectrophotometer. IR spectra were obtained as KBr disks with an ATI Mattson Genesis Series FTIR instrument.

Cyclic voltammetric measurements were carried out with an EG&G PAR model 283 potentiostat/galvanostat. An EG&G PAR K0264 single-compartment microcell was used with a silver/silver chloride reference electrode separated by a salt bridge from a Pt disk working electrode and a Pt wire auxiliary electrode. Acetonitrile (HPLC grade) was distilled before use, and $[NBu^n_4]PF_6$, twice recrystallized from ethanol and dried in vacuo, was used as the supporting electrolyte. Solutions containing ca. 10^{-3} M analyte (0.1 M electrolyte) were deaerated by purging with N_2. All $E_{1/2}$ values were calculated from $(E_{pa} + E_{pc})/2$ at a scan rate of 200 mV s^{-1}.

Synthesis of *N*-Methyl-4-[2-(4-pyridyl)ethynyl]pyridinium Iodide, [Mebpa$^+$]I. To a stirred solution of bpa (500 mg, 2.77 mmol) in diethyl ether (200 mL) was added methyl iodide (60 mL), and the solution was stirred for 24 h in the dark. The orange precipitate was filtered off and washed with diethyl ether. Yield: 345 mg (39%). ^{1}H NMR (200 MHz, D_2O): δ_H 8.79 (2 H, d, *J* = 6.7 Hz, C_5H_4N), 8.60 (2 H, d, *J* = 6.2 Hz, C_5H_4N), 8.10 (2 H, d, *J* = 6.8 Hz, C_5H_4N), 7.64 (2 H, d, *J* = 6.2 Hz, C_5H_4N), 4.37 (3 H, s, Me). IR: ν(C≡C) 2230m and 2186m cm^{-1}. Anal. Calcd (%) for $C_{13}H_{11}N_2I$: C, 48.47; H, 3.44; N, 8.70. Found: C, 48.30; H, 3.36; N, 8.58.

Synthesis of *N*-Methyl-4-[4-(4-pyridyl)buta-1,3-diynyl]pyridinium Iodide, [Mebpbd$^+$]I. This compound was prepared in a manner identical with that of [Mebpa$^+$]I but using bpbd (500 mg, 2.45 mmol) in place of bpa to afford an orange solid. Yield: 285 mg (34%). ^{1}H NMR (200 MHz, D_2O): δ_H 8.63 (2 H, d, *J* = 6.9 Hz, C_5H_4N), 8.40 (2 H, d, *J* = 6.3 Hz, C_5H_4N), 7.92 (2 H, d, *J* = 6.9 Hz, C_5H_4N), 7.43 (2 H, d, *J* = 6.3 Hz, C_5H_4N), 4.17 (3 H, s, Me). IR: ν(C≡C) 2220m and 2140m cm^{-1}. Anal. Calcd (%) for $C_{15}H_{11}N_2I$: C, 52.05; H, 3.20; N, 8.09. Found: C, 52.31; H, 2.81; N, 8.11.

Synthesis of *trans*-$[Ru^{III}(SO_4)(NH_3)_4(Mebpa^+)]Cl_2$. A mixture of *trans*-$[Ru^{II}Cl(NH_3)_4(SO_2)]Cl$ (100 mg, 0.329 mmol) and [Mebpa$^+$]I (159 mg, 0.494 mmol) was dissolved in Ar-degassed water (10 mL) and heated with stirring at ca. 45 °C under Ar for 30 min. Acetone was added to the brown solution, and a dark-brown precipitate was filtered off, washed with acetone, and dried to afford crude *trans*-$[Ru^{II}(NH_3)_4(SO_2)(Mebpa^+)]X_3$ (X = Cl and/or I). This material was dissolved in water (5 mL) and oxidized by the addition of a 1:1 mixture of 30% aqueous H_2O_2/2 M HCl (2 mL). After 10 min at room temperature, acetone was added, and the golden precipitate was filtered off, washed with acetone, and dried. Crude yield: 104 mg (59%). This material was used in subsequent reactions without further purification.

Synthesis of *trans*-$[Ru^{III}(SO_4)(NH_3)_4(Mebpbd^+)]Cl_2$. This compound was prepared in a manner identical with that of *trans*-$[Ru^{III}(SO_4)(NH_3)_4(Mebpa^+)]Cl_2$ by using [Mebpbd$^+$]I (171 mg, 0.494 mmol) in place of [Mebpa$^+$]I to afford a golden solid. Crude yield: 100 mg (55%).

Synthesis of $[Ru^{II}(NH_3)_5(Mebpa^+)](PF_6)_3$ (2). A solution of $[Ru^{II}(NH_3)_5(H_2O)][PF_6]_2$ (100 mg, 0.202 mmol) and [Mebpa$^+$]I (65 mg, 0.202 mmol) in Ar-degassed acetone (20 mL) was stirred at room temperature under Ar in the dark for 6 h. The addition of diethyl ether afforded a dark precipitate, which was filtered off, washed with diethyl ether, and dried. Purification was effected by precipitations from acetone/aqueous NH_4PF_6 and then from acetone/diethyl ether (three times) to afford a dark-blue-purple solid. Yield: 50 mg (30%). ^{1}H NMR (200 MHz, CD_3COCD_3): δ_H 9.09 (2 H, d, *J* = 6.5 Hz, C_5H_4N), 9.01 (2 H, d, *J* = 6.9 Hz, C_5H_4N), 8.31 (2 H, d, *J* = 6.7 Hz, C_5H_4N), 7.37 (2 H, d, *J* = 6.7 Hz, C_5H_4N), 4.58 (3 H, s, Me), 3.51 (3 H, s, *trans*-NH_3), 2.63 (12 H, s, 4 × *cis*-NH_3). IR: ν(C≡C) 2229m and 2195m cm^{-1}. Anal. Calcd (%) for $C_{13}H_{26}F_{18}N_7P_3Ru$: C, 19.13; H, 3.21; N, 12.01. Found: C, 19.69; H, 3.26; N, 11.45.

Synthesis of $[Ru^{II}(NH_3)_5(Mebpbd^+)](PF_6)_3$ (3). This compound was prepared in a manner identical with that of **2** by using [Mebpbd$^+$]I (70 mg, 0.202 mmol) in place of [Mebpa$^+$]I to afford a dark-blue-purple solid. Yield: 45 mg (27%). ^{1}H NMR (200 MHz, CD_3COCD_3): δ_H 9.13 (2 H, d, *J* = 6.5 Hz, C_5H_4N), 8.96 (2 H, d, *J* = 6.7 Hz, C_5H_4N), 8.36 (2 H, d, *J* = 6.7 Hz, C_5H_4N), 7.40 (2 H, d, *J* = 6.7 Hz, C_5H_4N), 4.68 (3 H, s, Me), 3.53 (3 H, s, *trans*-NH_3), 2.63 (12 H, s, 4 × *cis*-NH_3). IR: ν(C≡C) 2214m and 2157m cm^{-1}. Anal. Calcd (%) for $C_{15}H_{26}F_{18}N_7P_3Ru$: C, 21.44; H, 3.12; N, 11.67. Found: C, 19.41; H, 2.71; N, 10.35.

Synthesis of *trans*-$[Ru^{II}(NH_3)_4(py)(Mebpa^+)](PF_6)_3$ (5). A solution of *trans*-$[Ru^{III}(SO_4)(NH_3)_4(py)]Cl$ (100 mg, 0.263 mmol) in Ar-degassed water (6 mL) was reduced over zinc amalgam (3 lumps) with Ar agitation for 20 min. The resulting yellow/brown solution was filtered under Ar into a flask containing [Mebpa$^+$]I (127 mg, 0.394 mmol) in Ar-degassed water (4 mL), and the solution was stirred at room temperature in the dark under Ar for 6 h. The addition of solid NH_4PF_6 to the deep-blue-purple solution gave a dark precipitate, which was allowed to settle overnight in a refrigerator. The solid was filtered off, washed with water, and dried. Purification was effected by precipitation from acetone/diethyl ether, acetone/LiCl, acetone/aqueous NH_4PF_6, and finally acetone/diethyl ether (three times) to afford a dark-purple solid. Yield: 50 mg

(9) Curtis, J. C.; Sullivan, B. P.; Meyer, T. J. *Inorg. Chem.* **1983**, *22*, 224.
(10) Douglas, P. G.; Feltham, R. D.; Metzger, H. G. *J. Am. Chem. Soc.* **1971**, *93*, 84.
(11) Coe, B. J.; Harries, J. L.; Harris, J. A.; Brunschwig, B. S.; Coles, S. J.; Light, M. E.; Hursthouse, M. B. *Dalton Trans*. **2004**, 2935.
(12) Dello Ciana, L.; Haim, A. *J. Heterocycl. Chem.* **1984**, *21*, 607.
(13) Champness, N.; Khlobystov, A. N.; Majuga, A. G.; Schröder, M.; Zyk, N. V. *Tetrahedron Lett.* **1999**, *40*, 5413.

(22%). ^{1}H NMR (200 MHz, CD_3COCD_3): δ_H 9.13 (2 H, d, J = 6.7 Hz, C_5H_4N), 9.04 (2 H, d, J = 7.0 Hz, C_5H_4N), 8.90 (2 H, d, J = 5.3 Hz, $H^{2,6}$), 8.37 (2 H, d, J = 6.9 Hz, C_5H_4N), 8.00 (1 H, t, J = 7.5 Hz, H^4), 7.68−7.55 (4 H, C_5H_4N + $H^{3,5}$), 4.67 (3 H, s, Me), 2.80 (12 H, s, 4NH_3). IR: ν(C≡C) 2233m and 2198m cm^{-1}. Anal. Calcd (%) for $C_{18}H_{28}F_{18}N_7P_3Ru$: C, 24.61; H, 3.21; N, 11.16. Found: C, 26.67; H, 2.63; N, 9.54.

Synthesis of *trans*-[Ru^{II}(NH$_3$)$_4$(py)(Mebpbd$^+$)](PF$_6$)$_3$ (6). This compound was prepared and purified in a manner identical with that of **5** by using [Mebpbd$^+$]I (137 mg, 0.396 mmol) in place of [Mebpa$^+$]I to afford a dark-purple solid. Yield: 51 mg (21%). ^{1}H NMR (200 MHz, CD_3COCD_3): δ_H 9.14 (2 H, d, J = 6.6 Hz, C_5H_4N), 8.98 (2 H, d, J = 6.7 Hz, C_5H_4N), 8.87 (2 H, d, J = 5.1 Hz, $H^{2,6}$), 8.38 (2 H, d, J = 6.9 Hz, C_5H_4N), 7.97 (1 H, t, J = 7.6 Hz, H^4), 7.63−7.54 (4 H, C_5H_4N + $H^{3,5}$), 4.63 (3 H, s, Me), 2.79 (12 H, s, 4NH_3). IR: ν(C≡C) 2213m and 2151m cm^{-1}. Anal. Calcd (%) for $C_{20}H_{28}F_{18}N_7P_3Ru$: C, 26.62; H, 3.13; N, 10.86. Found: C, 29.36; H, 2.66; N, 9.20.

Synthesis of *trans*-[Ru^{II}(NH$_3$)$_4$(mim)(Mebpa$^+$)](PF$_6$)$_3$ (8). A solution of *trans*-[Ru^{III}(SO$_4$)(NH$_3$)$_4$(Mebpa$^+$)]Cl$_2$ (100 mg, 0.188 mmol) in Ar-degassed water (6 mL) was reduced over zinc amalgam (3 lumps) with Ar agitation for 20 min. The resulting purple solution was filtered under Ar into a flask containing *N*-methylimidazole (0.2 mL, 2.51 mmol) in Ar-degassed water (4 mL), and the solution was stirred at room temperature in the dark under Ar for 6 h. The crude product was precipitated by the addition of solid NH_4PF_6 to the deep-blue-purple solution, and purification was effected as for **5** to afford a dark-purple solid. Yield: 35 mg (21%). ^{1}H NMR (200 MHz, CD_3COCD_3): δ_H 9.09 (2 H, d, J = 6.6 Hz, C_5H_4N), 9.01 (2 H, d, J = 6.4 Hz, C_5H_4N), 8.35 (2 H, d, J = 6.9 Hz, C_5H_4N), 8.20 (1 H, s, $C_3N_2H_3$), 7.54−7.37 (4 H, C_5H_4N + $C_3N_2H_3$), 4.58 (3 H, s, C_5H_4NMe), 3.91 (3 H, s, $C_3N_2H_3Me$), 2.65 (12 H, s, 4NH_3). IR: ν(C≡C) 2229m and 2195m cm^{-1}. Anal. Calcd (%) for $C_{17}H_{29}F_{18}N_8P_3Ru$: C, 23.17; H, 3.32; N, 12.71. Found: C, 23.58; H, 3.36; N, 11.79.

Synthesis of *trans*-[Ru^{II}(NH$_3$)$_4$(mim)(Mebpbd$^+$)](PF$_6$)$_3$ (9). This compound was prepared and purified in a manner identical with that of **8** by using *trans*-[Ru^{III}(SO$_4$)(NH$_3$)$_4$(Mebpbd$^+$)]Cl$_2$ (100 mg, 0.180 mmol) in place of *trans*-[Ru^{III}(SO$_4$)(NH$_3$)$_4$(Mebpa$^+$)]Cl$_2$ to afford a dark-purple solid. Yield: 31 mg (19%). ^{1}H NMR (200 MHz, CD_3COCD_3): δ_H 9.14 (2 H, d, J = 6.6 Hz, C_5H_4N), 8.99 (2 H, d, J = 6.7 Hz, C_5H_4N), 8.37 (2 H, d, J = 6.7 Hz, C_5H_4N), 8.15 (1 H, s, $C_3N_2H_3$), 7.49−7.35 (4 H, C_5H_4N + $C_3N_2H_3$), 4.62 (3 H, s, C_5H_4NMe), 3.93 (3 H, s, $C_3N_2H_3Me$), 2.69 (12 H, s, 4NH_3). IR: ν(C≡C) 2212m and 2157m cm^{-1}. Anal. Calcd (%) for $C_{19}H_{29}F_{18}N_8P_3Ru$: C, 25.20; H, 3.23; N, 12.38. Found: C, 24.84; H, 3.11; N, 10.15.

Synthesis of *trans*-[Ru^{II}Cl(pdma)$_2$(bpbd)]PF$_6$ (12). A solution of *trans*-[Ru^{II}Cl(pdma)$_2$(NO)][PF$_6$]$_2$ (150 mg, 0.146 mmol) and NaN_3 (9.6 mg, 0.148 mmol) in acetone (5 mL) was stirred at room temperature for 2 h. Butan-2-one (15 mL) and bpbd (149 mg, 0.730 mmol) were added, and acetone was removed in vacuo. The solution was heated under reflux for 2 h and cooled to room temperature, and diethyl ether was added to afford an orange precipitate. The excess bpbd was removed by two precipitations from acetone/diethyl ether. The product was further purified by precipitation from acetone/aqueous NH_4PF_6 and then acetone/diethyl ether to afford an orange solid. Yield: 42 mg (27%). ^{1}H NMR (300 MHz, CD_3CN): δ_H 8.61 (2 H, d, J = 6.0 Hz, C_5H_4N), 8.17 (4 H, m, C_6H_4), 7.80 (4 H, m, C_6H_4), 7.42−7.39 (4 H, 2C_5H_4N), 6.88 (2 H, d, J = 6.9 Hz, C_5H_4N), 1.80 (12 H, s, 4AsMe), 1.61 (12 H, s, 4AsMe). IR: ν(C≡C) 2220m cm^{-1}. Anal. Calcd (%) for $C_{34}H_{40}As_4ClF_6N_2PRu$: C, 38.60; H, 3.81; N, 2.65. Found: C, 38.27; H, 3.70; N, 2.53.

Synthesis of *trans*-[Ru^{II}Cl(pdma)$_2$(Mebpbd$^+$)](PF$_6$)$_2$ (13). A solution of **12** (20 mg, 0.019 mmol) in DMF (1.5 mL) and methyl iodide (0.5 mL) was stirred at room temperature for 24 h. The excess methyl iodide was removed in vacuo, and the addition of aqueous NH_4PF_6 gave a dark-red precipitate, which was filtered off, washed with water, and dried. Purification was effected by precipitation from acetone/diethyl ether to afford a dark-red solid. Yield: 19 mg (83%). ^{1}H NMR (300 MHz, CD_3CN): δ_H 8.57 (2 H, d, J = 6.9 Hz, C_5H_4N), 8.17 (4 H, m, C_6H_4), 7.98 (2 H, d, J = 6.9 Hz, C_5H_4N), 7.80 (4 H, m, C_6H_4), 7.51 (2 H, d, J = 6.7 Hz, C_5H_4N), 6.89 (2 H, d, J = 6.9 Hz, C_5H_4N), 4.24 (3 H, s, C_5H_4NMe), 1.80 (12 H, s, 4AsMe), 1.61 (12 H, s, 4AsMe). IR: ν(C≡C) 2217m and 2154m cm^{-1}. Anal. Calcd (%) for $C_{35}H_{43}As_4ClF_{12}N_2P_2Ru$: C, 34.52; H, 3.56; N, 2.30. Found: C, 34.47; H, 3.57; N, 2.21.

Synthesis of *trans*-[Ru^{II}Cl(pdma)$_2$(bpeb)]PF$_6$ (14). This compound was prepared in a manner identical with that of **12** by using bpeb (200 mg, 0.713 mmol) in place of bpbd to afford an orange-red solid. Yield: 30 mg (22%). ^{1}H NMR (300 MHz, CD_3COCD_3): δ_H 8.62 (2 H, d, J = 6.2 Hz, C_5H_4N), 8.31 (4 H, m, C_6H_4(pdma)), 7.84 (4 H, m, C_6H_4(pdma)), 7.72 (2 H, d, J = 6.9 Hz, C_5H_4N), 7.63 (2 H, d, J = 8.6 Hz, C_6H_4), 7.60 (2 H, d, J = 8.6 Hz, C_6H_4), 7.47 (2 H, d, J = 6.0 Hz, C_5H_4N), 7.15 (2 H, d, J = 6.9 Hz, C_5H_4N), 1.91 (12 H, s, 4AsMe), 1.81 (12 H, s, 4AsMe). IR: ν(C≡C) 2219w cm^{-1}. Anal. Calcd (%) for $C_{40}H_{44}As_4ClF_6N_2PRu\cdot H_2O$: C, 41.71; H, 4.02; N, 2.43. Found: C, 41.80; H, 4.07; N, 2.20.

Synthesis of *trans*-[Ru^{II}Cl(pdma)$_2$(Mebpeb$^+$)][PF$_6$]$_2$ (15). This compound was prepared in a manner identical with that of **13** by using **14** (30 mg, 0.026 mmol) in place of **12** to afford a red solid. Yield: 25 mg (74%). ^{1}H NMR (300 MHz, CD_3COCD_3): δ_H 9.08 (2 H, d, J = 6.7 Hz, C_5H_4N), 8.32−8.26 (6 H, C_6H_4(pdma) + C_5H_4N), 7.83 (4 H, m, C_6H_4(pdma)), 7.73 (4 H, C_6H_4 + C_5H_4N), 7.61 (2 H, d, J = 8.5 Hz, C_6H_4), 7.05 (2 H, d, J = 6.7 Hz, C_5H_4N), 4.59 (3 H, s, C_5H_4NMe), 1.90 (12 H, s, 4AsMe), 1.80 (12 H, s, 4AsMe). IR: ν(C≡C) 2220m and 2179w cm^{-1}. Anal. Calcd (%) for $C_{41}H_{47}N_2As_4ClF_{12}P_2Ru\cdot 0.5Me_2CO$: C, 38.58; H, 3.81; N, 2.12. Found: C, 38.82; H, 4.13; N, 2.76.

X-ray Crystallography. Crystals of the salt *trans*-[Ru^{II}(NH$_3$)$_4$(py)(Mebpbd$^+$)](PF$_6$)$_3$·MeNO$_2$ (**6**·MeNO$_2$) were obtained by diffusion of diethyl ether vapor into a nitromethane solution at 4 °C. A red plate crystal of approximate dimensions 0.70 × 0.20 × 0.05 mm was attached to a Hamilton Cryoloop, using fomblin oil (perfluoropolymethylisopropyl ether) and mounted on a Bruker APEX CCD X-ray diffractometer. Cryocooling to 100 K was carried out by using an Oxford Cryosystems 700 series cryostream cooler. Intensity measurements were collected using graphite-monochromated Mo Kα radiation from a sealed X-ray tube with a monocapillary collimator. The intensities of the reflections of a sphere were collected with an exposure time per frame of 30 s. Data processing was carried out by using the Bruker *SAINT*[14] software package, and a semiempirical absorption correction was applied using *SADABS*.[14]

Crystals of complex salt **14** were obtained by slow diffusion of diethyl ether vapor into an acetonitrile solution. The orange, bladelike crystal chosen for diffraction studies had approximate dimensions of 0.44 × 0.08 × 0.04 mm. Data were collected on a Nonius Kappa CCD area-detector X-ray diffractometer controlled by the *Collect* software package.[15] The data were processed using

(14) *SAINT* (version 6.45) and *SADABS* (version 2.10); Bruker AXS Inc.: Madison, WI, 2003.
(15) Hooft, R. *Collect*, *Data collection software*; Nonius BV: Delft, The Netherlands, 1998.

Table 1. Crystallographic Data and Refinement Details for Complex Salts **6**·$MeNO_2$ and **14**

	6·$MeNO_2$	**14**
empirical formula	$C_{21}H_{31}F_{18}N_8O_2P_3Ru$	$C_{40}H_{44}As_4ClF_6N_2PRu$
fw	963.52	1133.94
cryst syst	monoclinic	monoclinic
space group	$P2_1/c$	$C2/c$
a/Å	8.912(3)	34.075(7)
b/Å	20.527(7)	9.3403(19)
c/Å	18.680(6)	32.136(6)
β/deg	92.498(6)	102.73(3)
U/Å^3	3413.8(19)	9977(3)
Z	4	8
T/K	100(2)	120(2)
μ/mm^{-1}	0.736	3.083
reflns collected	17196	13131
independent reflns (R_{int})	6005 (0.0676)	5391 (0.0760)
reflns with $I > 2\sigma(I)$	4092	2502
GOF on F^2	1.049	1.251
final R1, wR2 [$I > 2\sigma(I)$][a]	0.0630, 0.1513	0.1333, 0.3419
final R1, wR2 (all data)	0.0993, 0.1664	0.2359, 0.3956

[a] The structures were refined on F_o^2 using all data; the values of R1 are given for comparison with older refinements based on F_o with a typical threshold of $F_o > 4\sigma(F_o)$.

Denzo,[16] and a semiempirical absorption correction was applied using *SADABS*.[14]

The structures of both **6**·$MeNO_2$ and **14** were solved by direct methods and refined by full-matrix least squares on all F_o^2 data using *SHELXS-97* and *SHELXL-97*.[17] All non-hydrogen atoms were refined anisotropically. Hydrogen atoms were included in idealized positions using the riding model, with thermal parameters of 1.2 or 1.5 times those of the parent atoms. The crystal of **14** contained an unrefinable solvent (probably acetonitrile), which was removed by using the SQUEEZE procedure,[18] and disorder of the hexafluorophosphate anion was also observed. All other calculations for **6**·$MeNO_2$ were carried out using the *SHELXTL* package.[19] Crystallographic data and refinement details are presented in Table 1.

Hyper-Rayleigh Scattering (HRS). Details of the HRS experiment have been discussed elsewhere,[20] and the experimental procedure used was as previously described.[21] β values were determined by using the electric-field-induced second-harmonic generation (EFISHG) β_{1064} for *p*-nitroaniline (29.2×10^{-30} esu in acetonitrile)[22] as an external reference. All measurements were performed by using the 1064 nm fundamental of an injection-seeded, Q-switched Nd:YAG laser (Quanta-Ray GCR-250, 8 ns pulses, 7 mJ, 10 Hz). Dilute acetonitrile solutions ($10^{-5}-10^{-6}$ M) were used to ensure a linear dependence of $I_{2\omega}/I_\omega^2$ on the solute concentration, precluding the need for Lambert−Beer correction factors. Samples were filtered (Millipore, 0.45 μm), and none showed any fluorescence. One-dimensional hyperpolarizability is assumed, i.e., $\beta_{1064} = \beta_{zzz}$ (the z axis is the dipolar axis, defined by the Ru−pyridyl bond), and a relative error of ±15% is estimated.

Stark Spectroscopy. The Stark apparatus, experimental methods and data analysis procedure were exactly as previously reported.[11,23,24] Butyronitrile was used as the glassing medium, for which the local field correction f_{int} is estimated as 1.33.[23,24] The Stark spectrum for each compound was measured a minimum of three times using different field strengths, and the signal was always found to be quadratic in the applied field. A two-state analysis of the MLCT transitions gives

$$\Delta\mu_{ab}^2 = \Delta\mu_{12}^2 + 4\mu_{12}^2 \quad (1)$$

where $\Delta\mu_{ab}$ is the dipole moment difference between the diabatic states, $\Delta\mu_{12}$ is the observed (adiabatic) dipole moment difference, and μ_{12} is the transition dipole moment. Analysis of the Stark spectra in terms of the Liptay treatment[25] affords $\Delta\mu_{12}$, and the transition dipole moment μ_{12} can be determined from the oscillator strength f_{os} of the transition by

$$|\mu_{12}| = [f_{os}/(1.08 \times 10^{-5} E_{max})]^{1/2} \quad (2)$$

where E_{max} is the energy of the MLCT maximum (in wavenumbers). The degree of delocalization c_b^2 and electronic coupling matrix element H_{ab} for the diabatic states are given by

$$c_b^2 = \frac{1}{2}\left[1 - \left(\frac{\Delta\mu_{12}^2}{\Delta\mu_{12}^2 + 4\mu_{12}^2}\right)^{1/2}\right] \quad (3)$$

$$|H_{ab}| = |E_{max}(\mu_{12})/\Delta\mu_{ab}| \quad (4)$$

If the hyperpolarizability tensor β_0 has only nonzero elements along the MLCT direction, then this quantity is given by

$$\beta_0 = 3\Delta\mu_{12}(\mu_{12})^2/E_{max}^2 \quad (5)$$

A relative error of ±20% is estimated for the β_0 values derived from the Stark data and using eq 5, while experimental errors of ±10% are estimated for μ_{12}, $\Delta\mu_{12}$, and $\Delta\mu_{ab}$, ±15% for H_{ab}, and ±50% for c_b^2.

Results and Discussion

Synthetic Studies and General Characterization. The new complex salts **2**, **3**, **5**, **6**, **8**, **9**, **12**, and **13** (Figure 1) were synthesized by following established procedures in order to provide four series of systematically modified compounds together with the existing **1**,[26] **4**,[4c] **7**,[27] **10**,[28] and **11**.[11] The extended complexes in **14** and **15** were prepared to allow comparisons with **10**−**13**. Unfortunately, attempts at the preparation of the compound 1,6-bis(4-pyridyl)hexa-1,3,5-triyne and complexes thereof have thus far proven unsuccessful. All of the new compounds show diagnostic

(16) Otwinowski, Z.; Minor, W. *Methods Enzymol*. **1997**, *276*, 307.
(17) Sheldrick, G. M. *SHELXL 97, Programs for Crystal Structure Analysis* (release 97-2); University of Göttingen: Göttingen, Germany, 1997.
(18) van der Sluis, P.; Spek, A. L. *Acta Crystallogr., Sect A* **1990**, *46*, 194.
(19) *SHELXTL* (version 6.10); Bruker AXS Inc.: Madison, WI, 2000.
(20) (a) Clays, K.; Persoons, A. *Phys. Rev. Lett.* **1991**, *66*, 2980. (b) Hendrickx, E.; Clays, K.; Persoons, A. *Acc. Chem. Res.* **1998**, *31*, 675.
(21) Clays, K.; Persoons, A. *Rev. Sci. Instrum*. **1992**, *63*, 3285.
(22) Stähelin, M.; Burland, D. M.; Rice, J. E. *Chem. Phys. Lett*. **1992**, *191*, 245.
(23) Coe, B. J.; Harris, J. A.; Brunschwig, B. S. *J. Phys. Chem. A* **2002**, *106*, 897.
(24) Shin, Y. K.; Brunschwig, B. S.; Creutz, C.; Sutin, N. *J. Phys. Chem.* **1996**, *100*, 8157.
(25) (a) Liptay, W. In *Excited States*; Lim, E. C., Ed.; Academic Press: New York, 1974; Vol. 1, pp 129−229. (b) Bublitz, G. U.; Boxer, S. G. *Annu. Rev. Phys. Chem.* **1997**, *48*, 213.
(26) Coe, B. J.; Harris, J. A.; Harrington, L. J.; Jeffery, J. C.; Rees, L. H.; Houbrechts, S.; Persoons, A. *Inorg. Chem*. **1998**, *37*, 3391.
(27) Coe, B. J.; Chamberlain, M. C.; Essex-Lopresti, J. P.; Gaines, S.; Jeffery, J. C.; Houbrechts, S.; Persoons, A. *Inorg. Chem*. **1997**, *36*, 3284.
(28) Coe, B. J.; Beyer, T.; Jeffery, J. C.; Coles, S. J.; Gelbrich, T.; Hursthouse, M. B.; Light, M. E. *J. Chem. Soc., Dalton Trans*. **2000**, 797.

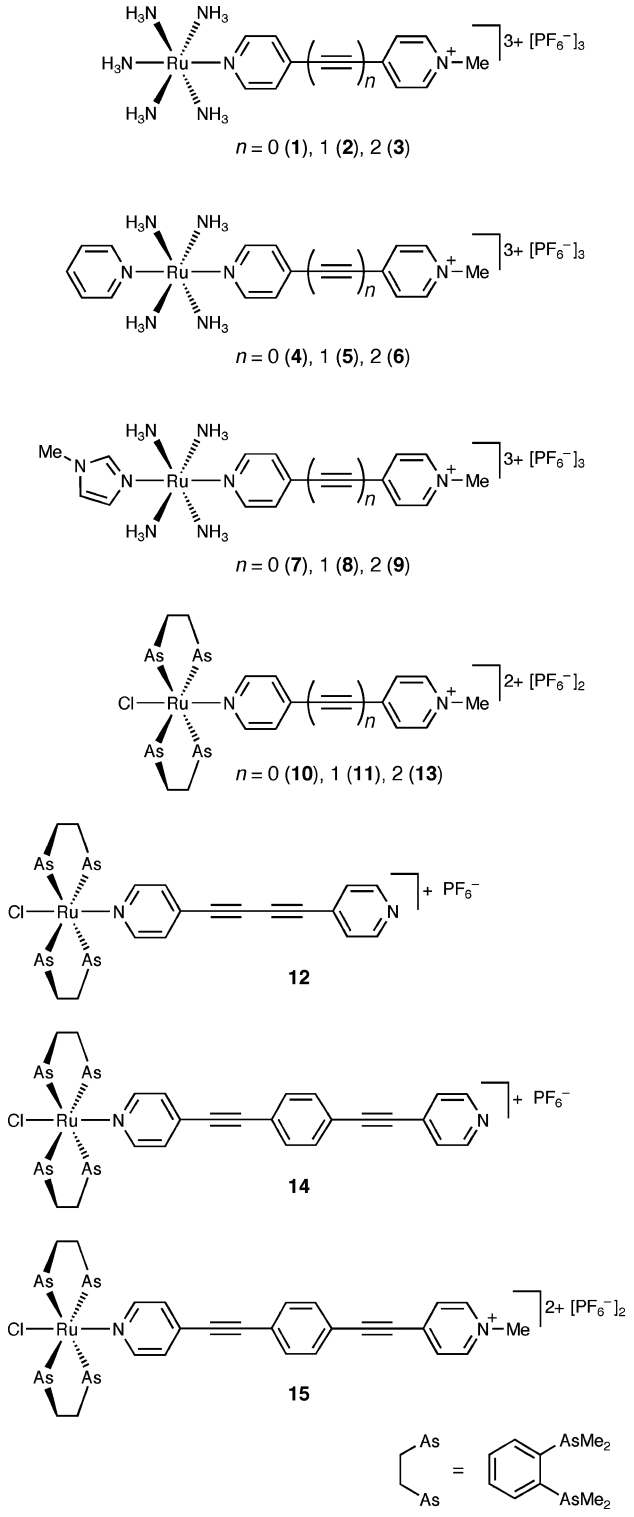

Figure 1. Chemical structures of the ruthenium(II) complex salts investigated.

^{1}H NMR spectra, and IR spectra confirm the presence of the ethynyl units. However, elemental analyses are only useful in providing further confirmation of the identity and purity for the complex salts containing the pdma ligand. Although we have previously reported satisfactory CHN analytical data for ruthenium(II) ammine complex salts,[4c,26,27] the new compounds **2**, **3**, **5**, **6**, **8**, and **9** repeatedly gave poor results (despite the use of V_2O_5 as a combustion aid), with satisfactory data being obtained only for **2** in one instance. The data obtained cannot be accounted for by invoking solvents of crystallization (water or acetone have been found previously in related samples), and although in most cases high C and low N percentages are observed, this behavior is not completely general or always reproducible. We therefore conclude that there is something inherently problematic about these ruthenium(II) ammine compounds featuring ethynyl groups with respect to elemental analyses. Nevertheless, given the clean NMR spectra obtained and the standard synthetic and purification procedures used, it is reasonable to suppose that the isolated materials are at least as pure as is required for the studies we describe herein.

Electronic Spectroscopy Studies. The UV−visible absorption spectra of salts **2**, **3**, **5**, **6**, **8**, **9**, and **12**−**15** have been measured in acetonitrile, and the results are presented in Table 2. Representative spectra of **13** and **15** are shown in Figure 2. These spectra feature intense absorptions in the UV region due to $\pi \rightarrow \pi^*$ intraligand charge-transfer (ILCT) transitions, together with intense, broad $d(Ru^{II}) \rightarrow \pi^*(L_A)$ (L_A = pyridyl ligand) visible MLCT bands. Data for the MLCT bands are also collected in Table 3, together with data for the other compounds discussed in this work.[4c,11,26−28]

Extension of π-conjugated systems normally leads to red-shifting of ICT and MLCT bands. Indeed, both experimental and theoretical studies with purely organic D−A diphenylpolyyne chromophores show that this is the case, although the shifts are not always large.[29] However, in the three ammine series within **1**−**9**, the MLCT bands show slight blue shifts as the number of ethynyl units *n* increases from 0 to 2. Such contrasting behavior between related purely organic and metal-containing chromophores is strongly reminiscent of our previous studies with related polyenyl systems.[30] In the latter complexes, blue-shifting of the MLCT bands with extension beyond a single (*E*)-ethenyl linkage is attributable to decreased D−A electronic coupling and consequent increased ILCT character as the conjugated system extends.[30] For any given L_A, the MLCT E_{max} decreases as the trans ligand changes in the order py < NH_3 < mim, correlating with mim being the most electron-donating of the three trans ligands. Such red-shifting of the MLCT bands is attributable to destabilization of the Ru-based HOMOs, and a similar trend has been observed previously in related ruthenium(II) ammine complexes.[4c,26,31] Methylation of the uncoordinated pyridyl nitrogens in **12** and **14** (to form **13** and **15**, respectively) leads to red-shifting of the MLCT bands, as the electron-accepting strength of L_A increases. However, this effect is much more pronounced on moving from **12** to **13** (ΔE_{max} = 0.16 eV) than between **14** and **15** (ΔE_{max} = 0.05 eV), showing that the π-electronic

(29) (a) Stiegman, A. E.; Miskowski, V. M.; Perry, J. W.; Coulter, D. R. *J. Am. Chem. Soc.* **1987**, *109*, 5884. (b) Stiegman, A. E.; Graham, E.; Perry, K. J.; Khundkar, L. R.; Cheng, L.-T.; Perry, J. W. *J. Am. Chem. Soc.* **1991**, *113*, 7658. (c) Dehu, C.; Meyers, F.; Brédas, J. L. *J. Am. Chem. Soc.* **1993**, *115*, 6198.
(30) Coe, B. J.; Harris, J. A.; Brunschwig, B. S.; Garín, J.; Orduna, J.; Coles, S. J.; Hursthouse, M. B. *J. Am. Chem. Soc.* **2004**, *126*, 10418.
(31) Coe, B. J.; Harris, J. A.; Asselberghs, I.; Persoons, A.; Jeffery, J. C.; Rees, L. H.; Gelbrich, T.; Hursthouse, M. B. *J. Chem. Soc., Dalton Trans.* **1999**, 3617.

Table 2. UV−Visible and Electrochemical Data for Complex Salts **2**, **3**, **5**, **6**, **8**, **9**, and **12**−**15** in Acetonitrile

				E, V vs Ag−AgCl (ΔE_p, mV)[b]	
salt	λ_{max},[a] nm (ϵ, M^{-1} cm^{-1})	E_{max},[a] eV	assignment	$E_{1/2}$[Ru$^{III/II}$]	E_{pc}[c]
[Ru^{II}(NH$_3$)$_5$(Mebpa$^+$)][PF$_6$]$_3$ (**2**)	586 (19 000)	2.12	d → π*	0.50 (100)	−0.83
	296 (27 500)	4.19	π → π*		
[Ru^{II}(NH$_3$)$_5$(Mebpbd$^+$)][PF$_6$]$_3$ (**3**)	580 (20 500)	2.14	d → π*	0.49 (85)	−0.73
	324 (23 000)	3.83	π → π*		−1.49
	306sh (20 500)	4.05	π → π*		
	268 (24 000)	4.63	π → π*		
	254sh (22 500)	4.88	π → π*		
trans-[Ru^{II}(NH$_3$)$_4$(py)(Mebpa$^+$)][PF$_6$]$_3$ (**5**)	558 (15 500)	2.22	d → π*	0.65 (80)	−0.81
	286 (40 500)	4.34	π → π*		
trans-[Ru^{II}(NH$_3$)$_4$(py)(Mebpbd$^+$)][PF$_6$]$_3$ (**6**)	546 (18 000)	2.27	d → π*	0.65 (100)	−0.73
	345sh (18 500)	3.59	π → π*		−1.42
	324 (22 500)	3.83	π → π*		
	304sh (20 000)	4.08	π → π*		
	268 (26 000)	4.63	π → π*		
	258sh (25 500)	4.81	π → π*		
trans-[Ru^{II}(NH$_3$)$_4$(mim)(Mebpa$^+$)][PF$_6$]$_3$ (**8**)	596 (14 000)	2.08	d → π*	0.48 (115)	−0.82
	284 (33 200)	4.37	π → π*		
trans-[Ru^{II}(NH$_3$)$_4$(mim)(Mebpbd$^+$)][PF$_6$]$_3$ (**9**)	586 (16 500)	2.12	d → π*	0.46 (115)	−0.75
	324 (19 000)	3.83	π → π*		
	304sh (17 500)	4.08	π → π*		
	270 (21 000)	4.59	π → π*		
trans-[Ru^{II}Cl(pdma)$_2$(bpbd)]PF$_6$ (**12**)	454 (8800)	2.73	d → π*	1.15 (70)	−1.28
	324 (17 300)	3.83	π → π*		
	302 (23 000)	4.11	π → π*		
	286 (23 400)	4.34	π → π*		
	272 (28 800)	4.56	π → π*		
	240 (36 200)	5.17	π → π*		
trans-[Ru^{II}Cl(pdma)$_2$(Mebpbd$^+$)][PF$_6$]$_2$ (**13**)	482 (10 700)	2.57	d → π*	1.14 (70)	−0.69
	342 (13 800)	3.63	π → π*		
	320 (16 100)	3.88	π → π*		
	298 (15 500)	4.16	π → π*		
	280sh (18 000)	4.43	π → π*		
	264 (20 000)	4.70	π → π*		
trans-[Ru^{II}Cl(pdma)$_2$(bpeb)]PF$_6$ (**14**)	438 (15 000)	2.83	d → π*	1.10 (75)	−1.47
	320 (39 200)	3.88	π → π*		
trans-[Ru^{II}Cl(pdma)$_2$(Mebpeb$^+$)][PF$_6$]$_2$ (**15**)	446 (15 500)	2.78	d → π*	1.11 (75)	−0.89
	354 (37 400)	3.50	π → π*		−1.56
	344sh (35 900)	3.60	π → π*		
	276 (24 100)	4.49	π → π*		

[a] Solutions of ca. (3−8) × 10^{-5} M. [b] Solutions of ca. 10^{-3} M in analyte and 0.1 M in [NBu$^n_4$]PF$_6$ at a Pt disk working electrode with a scan rate of 200 mV s^{-1}. Ferrocene internal reference $E_{1/2}$ = 0.43 V and ΔE_p = 70 mV. [c] For an irreversible reduction process.

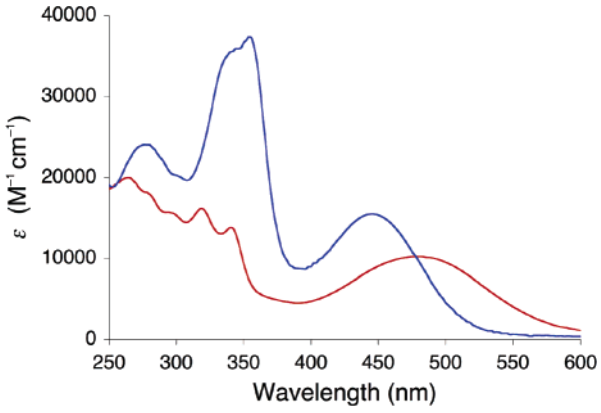

Figure 2. UV−visible absorption spectra of salts **13** (red) and **15** (blue) in acetonitrile at 295 K.

coupling between the Ru^{II} center and pyridyl/*N*-methylpyridinium unit is greatly weakened upon insertion of a 1,4-phenylene unit into the conjugated bridge. This structural change also leads to a substantial blue shift in the MLCT band of 0.21 eV on moving from **13** to **15** (Figure 2) but a smaller corresponding shift of 0.10 eV for the unmethylated pair **12** and **14**.

Within the pdma-containing series **10**, **11**, and **13**, the E_{max} values exhibit a different trend when compared with the corresponding ammine species. Thus, E_{max} decreases very slightly as n increases from 0 to 1 but then increases on moving to n = 2. The E_{max} values of the ammine complexes (in **1**−**9**) are lower by as much as ca. 0.5 eV when compared with those of the related pdma complexes (in **10**, **11**, and **13**) because the ammine centers are more efficient electron donors than *trans*-{Ru^{II}Cl(pdma)$_2$}$^+$. The intensities of these transitions are also consistently higher for the ammine complexes, indicative of more effective D−A orbital overlap. Such differences have been noted previously in related complexes.[11,28]

Electrochemical Studies. The new complex salts **2**, **3**, **5**, **6**, **8**, **9**, and **12**−**15** were studied by cyclic voltammetry in acetonitrile, and the results are presented in Table 2. All of the complexes show reversible or quasi-reversible Ru$^{III/II}$ oxidation waves, together with irreversible L$_A$-based reduction processes. Selected electrochemical data are also collected in Table 3, together with that for the other compounds discussed in this work.[4c,11,26−28]

Table 3. MLCT Absorption and Selected Cyclic Voltammetric Data for Complex Salts **1**−**15** in Acetonitrile

				E, V vs Ag−AgCl[b]	
salt	λ_{max},[a] nm	E_{max},[a] eV	ϵ,[a] M^{-1} cm^{-1}	$E_{1/2}[Ru^{III/II}]$	reduction of L_A
1[c]	590	2.10	15 800	0.48	−0.89
2	586	2.12	19 000	0.50	−0.83[d]
3	580	2.14	20 500	0.49	−0.73[d]
4[e]	566	2.19	17 200	0.66	−0.84
5	558	2.22	15 500	0.65	−0.81[d]
6	546	2.27	18 000	0.65	−0.73[d]
7[f]	602	2.06	16 200	0.49	−0.86
8	596	2.08	14 000	0.48	−0.82[d]
9	586	2.12	16 500	0.46	−0.75[d]
10[g]	486	2.55	8 300	1.14	−0.74
11[h]	488	2.54	11 500	1.15	−0.98[d]
12	454	2.73	8 800	1.15	−1.28[d]
13	482	2.57	10 700	1.14	−0.69[d]
14	438	2.83	15 000	1.10	−1.47[d]
15	446	2.78	15 500	1.11	−0.89[d]

[a] Solutions of ca. (3−8) × 10^{-5} M. [b] Solutions of ca. 10^{-3} M in analyte and 0.1 M in $[NBu^n_4]PF_6$ at a Pt bead/disk working electrode with a scan rate of 200 mV s^{-1}. Ferrocene internal reference $E_{1/2}$ = 0.43 V. [c] Reference 26. [d] For an irreversible reduction process. [e] Reference 4c. [f] Reference 27. [g] Reference 28. [h] Reference 11.

The $Ru^{III/II}$ $E_{1/2}$ values of the pentaammine (**1**−**3**) and tetraammine mim series (**7**−**9**) are very similar but lower by ca. 150 mV when compared with those of the corresponding py-containing series (**4**−**6**). This difference reflects the lower basicity of py as opposed to NH_3 or mim and is also manifested in the MLCT energies. Within the three ammine series, for a given trans ligand, $E_{1/2}[Ru^{III/II}]$ is essentially independent of the nature of L_A, showing that the π-acceptor strength of the latter has no significant influence on the energy of the Ru-based HOMO. Such behavior is also observed in the pdma-containing series (**10**, **11**, and **13**), which also have much higher $Ru^{III/II}$ potentials than all of their ammine counterparts because of the greater electron-richness of the metal centers in the latter.[11,28]

Although all of the ethynyl-containing complexes show only irreversible L_A-based reductions, their E_{pc} values do show a general trend of increasing with *n*, indicating that the ligands become easier to reduce with extension of the conjugated bridge. This observation is consistent with the fact that an extra electron is expected to be more effectively delocalized over a longer π system. The red shifts of the MLCT bands on methylation of the uncoordinated pyridyl nitrogens in **12** and **14** (to form **13** and **15**, respectively) are not accompanied by any significant changes in the $Ru^{III/II}$ potentials, but large increases in E_{pc} are observed. Hence, these decreases in E_{max} can be attributed solely to stabilization of the L_A-based LUMOs.

Crystallographic Studies. Single-crystal X-ray structures were obtained for salts **6**·$MeNO_2$ and **14**, and representations of the molecular structures of the complex cations are shown in Figures 3 and 4. Selected interatomic distances and angles are presented in Table 4. The crystals of **14** were found to be extremely sensitive toward loss of solvent (presumably acetonitrile), and the quality of this structure is unfortunately not very high.

The dihedral angle between the pyridyl and pyridinium rings in **6**·$MeNO_2$ is 18.32(0.21)°. In addition, there is

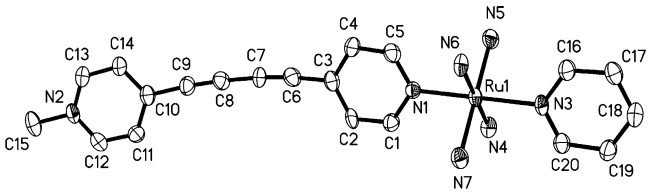

Figure 3. Structural representation of the complex cation in the salt **6**·$MeNO_2$ (50% probability ellipsoids).

substantial bending of the buta-1,3-dienyl unit, with angles as follows: C3−C6−C7 = 174.1(7)°, C6−C7−C8 = 173.9(7)°, C7−C8−C9 = 172.9(8)°, and C8−C9−C10 = 174.6(8)°. Although the crystal structure of bpbd reveals a completely planar molecule,[32] similarly distorted buta-1,3-dienyl units have been found in coordination complexes of this compound.[33] The trans-coordinated pyridyl rings are almost coplanar, forming a dihedral angle of 4.79(0.22)°, and essentially bisect the (ammine)N−Ru−N(ammine) angles. The bpeb ligand in **14** displays a relatively planar conformation, with dihedral angles as follows: coordinated pyridyl ring−phenylene ring = 9.35(1.11)° and phenylene ring−uncoordinated pyridyl ring = 8.59(1.14)°. It is, however, worth noting that such dihedral angles in complexes of these types do not give meaningful indications of the effectiveness of D−A electronic communication but rather are likely to result largely from solid-state effects.[28] The adoption of the centrosymmetric space groups $P2_1/c$ and $C2/c$ by **6**·$MeNO_2$ and **14**, respectively, precludes any significant bulk quadratic NLO effects from these particular materials.

HRS Studies. The β responses of the new complex salts **2**, **3**, **5**, **6**, **8**, **9**, **13**, and **15** were measured in acetonitrile by using the HRS technique[20,21] with a 1064 nm Nd:YAG laser fundamental. Estimated static first hyperpolarizabilities, denoted as β_0[H], were obtained by application of the two-state model (using the E_{max} values shown in Table 3),[34] and the results are presented in Table 5, together with data for the other compounds discussed in this work.[4c,26,27] It is worth noting that these HRS results for **10**, **11**, **13**, and **15** constitute the first such data to be reported for *trans*-$\{Ru^{II}Cl(pdma)_2\}^+$-based chromophores.

For the two ammine series **1**−**3** and **7**−**9**, β_0[H] increases as *n* increases from 0 to 1 but then decreases upon further extension of the conjugation to *n* = 2. However, the difference between the values for **8** and **9** is within the experimental error. Previous EFISHG studies with purely organic D−A diphenylpolyynes have shown that the β responses do not increase appreciably upon extension from *n* = 1 to 2.[29b] INDO/SCI calculations on such compounds verify the experimental results and also indicate that the two-state model holds well for such chromophores, although it breaks down upon moving to *n* = 3 systems.[29c] The limited comparable EFISHG data available for 4,4′-disubstituted

(32) Allan, J. R.; Barrow, M. J.; Beaumont, P. C.; Macindoe, L. A.; Milburn, G. H. W.; Werninck, A. R. *Inorg. Chim. Acta* **1988**, *148*, 85.
(33) For examples, see: (a) Lin, J. T.; Sun, S.-S.; Wu, J. J.; Lee, L.; Lin, K.-J.; Huang, Y. F. *Inorg. Chem.* **1995**, *34*, 2323. (b) Zaman, Md. B.; Smith, M. D.; zur Loye, H.-C. *Chem. Mater.* **2001**, *13*, 3534.
(34) (a) Oudar, J. L.; Chemla, D. S. *J. Chem. Phys.* **1977**, *66*, 2664. (b) Oudar, J. L. *J. Chem. Phys.* **1977**, *67*, 446.

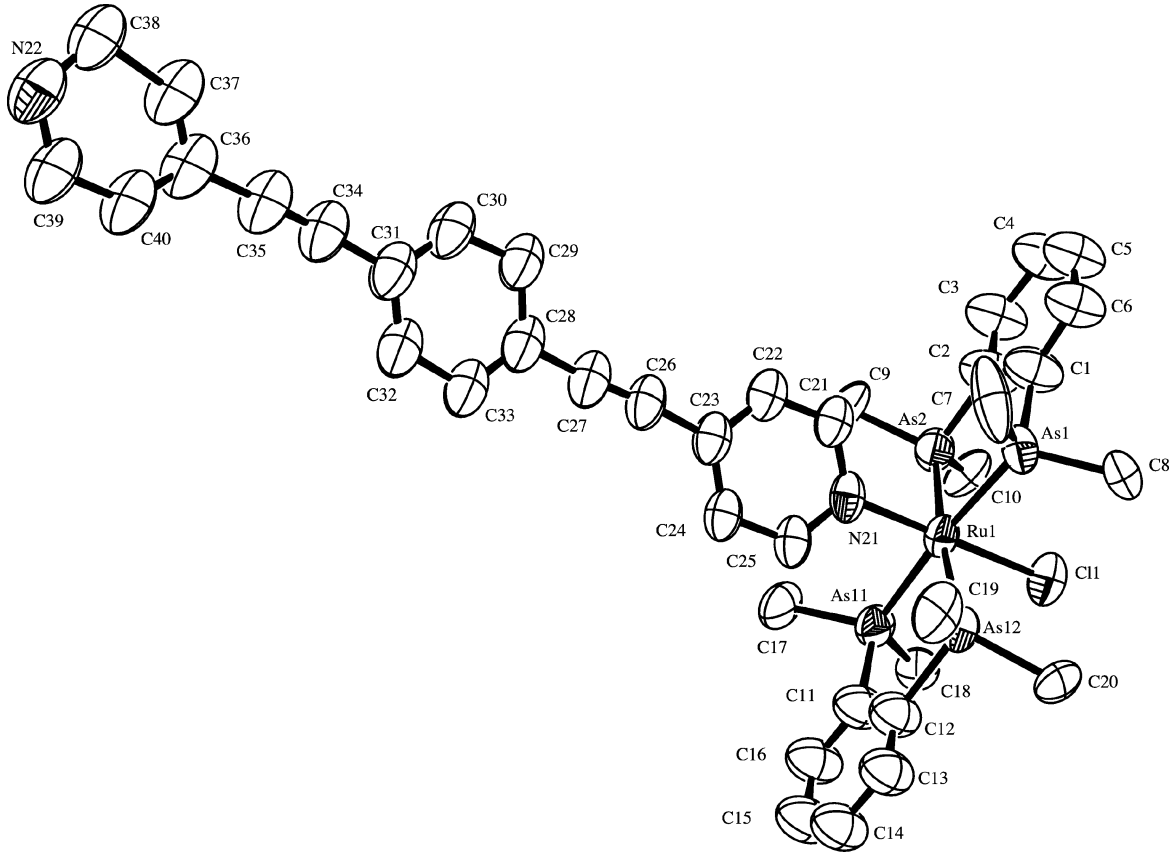

Figure 4. Structural representation of the complex cation in the salt **14** (50% probability ellipsoids).

Table 4. Selected Interatomic Distances (Å) and Angles (deg) for Salts **6**·$MeNO_2$ and **14**

	6·$MeNO_2$		
Ru1−N1	2.051(5)	Ru1−N6	2.132(6)
Ru1−N3	2.087(5)	Ru1−N7	2.135(5)
Ru1−N4	2.129(6)	Ru1−N5	2.136(5)
N1−Ru1−N3	178.8(2)	N4−Ru1−N7	93.1(2)
N1−Ru1−N4	89.9(2)	N6−Ru1−N7	86.4(2)
N3−Ru1−N4	89.0(2)	N1−Ru1−N5	89.49(19)
N1−Ru1−N6	90.32(19)	N3−Ru1−N5	89.98(19)
N3−Ru1−N6	90.8(2)	N4−Ru1−N5	87.2(2)
N4−Ru1−N6	179.5(2)	N6−Ru1−N5	93.3(2)
N1−Ru1−N7	90.81(19)	N7−Ru1−N5	179.6(2)
N3−Ru1−N7	89.71(19)		
	14		
Ru1−Cl1	2.418(6)	Ru1−As11	2.413(3)
Ru1−N21	2.080(17)	Ru1−As2	2.416(3)
Ru1−As1	2.410(3)	Ru1−As12	2.415(3)
N21−Ru1−As1	93.7(5)	As11−Ru1−As2	96.33(10)
N21−Ru1−As11	91.1(5)	As12−Ru1−As2	174.74(11)
As1−Ru1−As11	174.81(11)	N21−Ru1−Cl1	179.1(4)
N21−Ru1−As1	92.6(5)	As1−Ru1−Cl1	86.84(17)
As1−Ru1−As12	93.11(10)	As11−Ru1−Cl1	88.39(17)
As11−Ru1−As12	84.70(11)	As12−Ru1−Cl1	88.16(17)
N21−Ru1−As2	92.6(5)	As2−Ru1−Cl1	86.71(17)
As1−Ru1−As2	85.43(11)		

biphenyls show that such $n = 0$ molecules have β values similar to those of the corresponding diphenylpolyyne derivatives.[7] For the py-containing salts **4**−**6**, β_0[H] apparently decreases steadily as n increases, although because of the proximity of the MLCT λ_{max} to the second-harmonic wavelength (Table 3), β_0[H] for **6** is strongly underestimated. Nevertheless, the observation that **4**−**6** have smaller β_0[H] values when compared with their pentaammine or mim-containing counterparts is consistent with py being the least electron-donating of the trans ligands, as evidenced by both the MLCT and electrochemical data.

For the pdma-containing series **10**, **11**, and **13**, β_0[H] does not change as n is increased from 0 to 1 but increases significantly as the conjugation is extended further to $n = 2$. At present, we cannot explain why these complexes behave differently from their ammine counterparts, but it is likely that the greatly differing electron donor abilities of the Ru^{II} centers may be important. The β_0[H] values for **13** and **15** are very similar, indicating that insertion of a 1,4-phenylene unit into the conjugated bridge does not significantly affect the NLO response. **10**, **11**, and **13** generally have somewhat lower β_0[H] values when compared with their ammine counterparts, attributable to the less effective π-electron-donating abilities of the *trans*-{Ru^{II}Cl(pdma)$_2$}$^+$ center.[11,28]

Stark Spectroscopic Studies. We have studied the MLCT bands of the new complex salts **2**, **3**, **5**, **6**, **8**, **9**, **13**, and **15** by using Stark spectroscopy in butyronitrile glasses at 77 K, and the results are presented in Table 5, together with data for the other compounds discussed in this work.[4c,11,23] Representative absorption and Stark spectra and the spectral components for **2** and **3** are presented in Figure 5.

As observed previously with related ruthenium(II) ammine and pdma-containing chromophores,[4c,11,23] E_{max} decreases upon moving from an acetonitrile solution to a butyronitrile glass, although the observed red shifts are less pronounced in the pdma complexes. Interestingly, the trends in E_{max} for the three ammine series within **1**−**9** measured in 77 K glasses

Table 5. MLCT Absorption, Stark Spectroscopic, and HRS Data for the Complex Salts **1**−**11**, **13**, and **15**

salt	n	λ_{max},[a] nm	E_{max},[a] eV	f_{os}[a]	μ_{12},[b] D	$\Delta\mu_{12}$,[c] D	$\Delta\mu_{ab}$,[d] D	c_b^2 [e]	H_{ab},[f] cm^{-1}	β_0[S],[g] 10^{-30} esu	β_{1064},[h] 10^{-30} esu	β_0[H],[i] 10^{-30} esu
1[j,k]	0	645	1.92	0.20	5.2	13.8	17.3	0.10	4700	120	750	123
2	1	648	1.91	0.25	5.9	19.6	22.9	0.07	4000	216	1136	169
3	2	664	1.87	0.28	6.3	23.4	26.6	0.06	3600	308	884	117
4[l]	0	611	2.03	0.29	6.1	16.2	20.3	0.10	4900	171	899	85
5	1	618	2.01	0.24	5.6	19.8	22.7	0.06	4000	178	1077	78
6	2	627	1.98	0.32	6.6	25.7	28.9	0.05	3600	331	1280	50
7[k,m]	0	658	1.88	0.22	5.5	17.1	20.3	0.08	4100	170	523	100
8	1	661	1.88	0.24	5.8	21.6	24.5	0.06	3600	241	1143	200
9	2	667	1.86	0.34	7.0	27.6	31.0	0.05	3400	457	1300	193
10[n]	0	491	2.53	0.41	6.6	14.3	19.4	0.13	6900	113	341	45
11[n]	1	509	2.44	0.38	6.4	18.2	22.3	0.09	5600	146	359	45
13	2	506	2.45	0.22	4.9	22.8	24.8	0.04	3900	106	490	70
15		472	2.63	0.29	5.4	23.2	25.6	0.05	4500	114	310	76

[a] Measured in butyronitrile glasses at 77 K. [b] Calculated from eq 2. [c] Calculated from $f_{int}\Delta\mu_{12}$ using $f_{int} = 1.33$. [d] Calculated from eq 1. [e] Calculated from eq 3. [f] Calculated from eq 4. [g] Calculated from eq 5. [h] Obtained from 1064 nm HRS measurements in acetonitrile solutions at 295 K. [i] Derived from β_{1064} by application of the two-state model.[34] [j] Reference 26. [k] Reference 23. [l] Reference 4c. [m] Reference 27. [n] Data taken in part from ref 11.

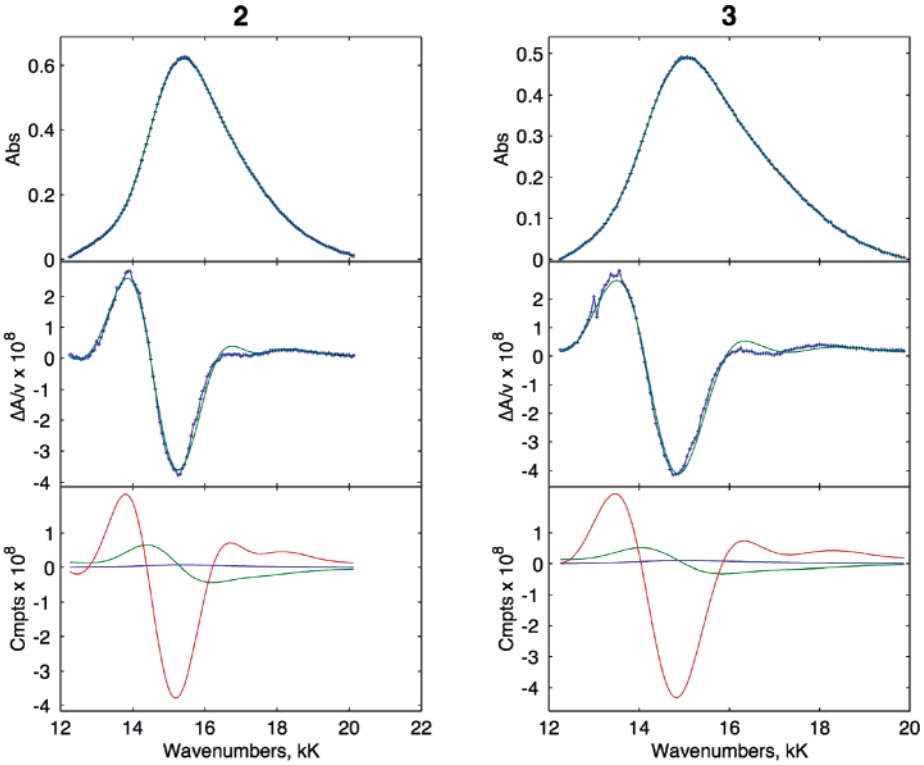

Figure 5. Absorption and electroabsorption spectra and calculated fits for the complex salts **2** and **3** in an external electric field of 1.84×10^7 V m^{-1}. Top panel: absorption spectrum. Middle panel: electroabsorption spectrum, experimental (blue) and fits (green) according to the Liptay equation.[25] Bottom panel: contribution of zeroth (blue), first (green), and second (red) derivatives of the absorption spectrum to the calculated fits.

are quite different from those observed in solutions at 295 K. In butyronitrile glasses, E_{max} decreases as n increases, whereas in acetonitrile solutions, an opposite behavior is observed. Generally, both f_{os} and μ_{12} increase with n, although **5** has unexpectedly low values for both parameters. As expected, both $\Delta\mu_{12}$ and $\Delta\mu_{ab}$ increase with the length of L_A. In contrast, H_{ab} and c_b^2 decrease as n increases, indicating decreasing D−A electronic coupling as the π bridge extends. Within all three ammine series, the β_0[S] values derived by using eq 5 increase with n, such that the NLO responses for the Mebpbd$^+$ complexes are at least twice as large as those of their MeQ$^+$ analogues. This trend is attributable to decreases in E_{max}, together with increases in both $\Delta\mu_{12}$ and μ_{12}. For a given L_A, the mim complex generally has the largest β_0[S], corresponding with mim being the strongest electron donor of the trans ligands.

Within the pdma-containing series **10**, **11**, and **13**, in contrast to the ammines, the E_{max} values exhibit the same general trend when measured in butyronitrile glasses or in acetonitrile solutions. At 77 K, E_{max} decreases as n increases from 0 to 1 but increases slightly upon moving to $n = 2$. Again, in contrast with the ammines, f_{os} and μ_{12} for **10**, **11**, and **13** decrease as n increases. However, the dependencies of $\Delta\mu_{12}$, $\Delta\mu_{ab}$, c_b^2, and H_{ab} on n are the same in both pdma- and ammine-containing chromophores. Most importantly, the derived β_0[S] response peaks at $n = 1$ (**11**), so the pdma complexes differ also from their ammine counterparts in this regard, an observation that can be traced to the contrasting

behavior of the MLCT bands for the two types of complexes. As with the HRS results, the differing electron-donor abilities of the ruthenium(II) ammine and pdma centers are probably important in this context. In a logical fashion, the weaker electron-donating strength of the *trans*-{Ru^{II}Cl(pdma)$_2$}$^+$ center is manifested in smaller NLO responses when compared with any of the corresponding ammine complexes of a given L_A, and the β_0[S] values for the Mebpbd$^+$ complexes are at least 3 times larger with the ammine centers. Given that the HRS and Stark measurements were carried out under quite different experimental conditions and also that alternate versions of eq 5 exist that would afford β_0[S] values differing by factors of 2 or 0.5,[35] a comparison between the NLO responses obtained from these two techniques is of limited utility. Nevertheless, in agreement with the HRS results, **13** and **15** have very similar β_0[S] values. It is hence clear that the addition of a 1,4-phenylene bridging unit does not greatly affect the NLO response, although a significant gain in visible transparency is achieved by this structural modification (Figure 2).

A comparison of the H_{ab} values obtained for **11**, **13**, and **15** shows a decrease upon moving from an ethynyl to a buta-1,3-diynyl linkage but then an increase upon insertion of a 1,4-phenylene bridging unit. Interestingly, this behavior contrasts with that observed in purely organic mixed-valence triarylamine cations where the Hush coupling energies V derived from measurements on intervalence charge-transfer bands follow the trend of decreasing upon moving from a −C≡C− to a −C≡C−C≡C− to a −C≡C-4-C$_6$H$_4$−C≡C− linkage (the respective values in cm^{-1} are 1200, 710, and 500).[36] Note, however, that comparisons between V and H_{ab} values should be made only with caution because these parameters are derived via quite different approaches.

Further Comparisons with Diphenylpolyyne Chromophores. As found previously with related polyenyl systems,[30] the data presented here clearly show that the optical properties of the new ethynyl-containing complex species differ somewhat from those of the closest known corresponding purely organic molecules, i.e., diphenylpolyynes. Furthermore, the behavior of the complexes is strongly medium-dependent. The blue shifting of the MLCT absorptions in acetonitrile solutions is replaced by red shifting in butyronitrile glasses, and the latter resembles more closely the behavior of the purely organic compounds. Both the HRS and Stark measurements on the complexes show that β_0 varies (often substantially) with n, in contrast with D−A diphenylpolyyne chromophores. Although we have not yet carried out any molecular orbital calculations on our ethynyl-containing complexes, it appears likely that the differences between the two types of molecules originate from variations in orbital structures and D−A electronic coupling, as found in the related polyenyl species.[30] However, the temperature/medium dependence shown by the new complexes is intriguing and worthy of further investigations.

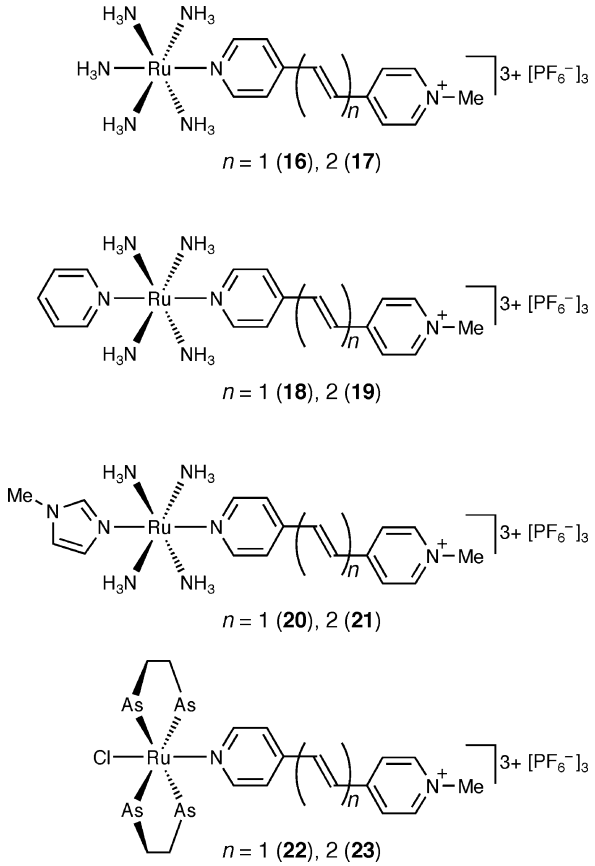

Figure 6. Chemical structures of the ruthenium(II) ethenyl-containing complex salts investigated.[4b,c,11,31]

Comparisons between Ethynyl-Containing and Analogous Ethenyl Complexes. We have previously reported studies on ruthenium(II) ammine and *trans*-{Ru^{II}Cl(pdma)$_2$}$^+$ complexes of pyridyl−pyridinium polyenyl ligands.[4b,c,11] Unusual linear and NLO behavior is observed for such compounds, both in butyronitrile glasses and in acetonitrile solutions, with the MLCT bands blue-shifting after $n = 1$ and β_0 peaking at $n = 2$. The ability to draw quantitative comparisons between these known complexes and the new ethynyl-containing species is a major objective of the present study. To our knowledge, Stark spectroscopy has not been used previously to compare ethenyl and ethynyl chromophores of any sort. Selected data for **1**−**11** and **13**, together with those for the related complex salts **16**−**23** (Figure 6), are collected in Table 6, with the data arranged such that each ethynyl-containing complex appears directly below its ethenyl analogue. Representative UV−visible spectra for salts **3** and **17** are shown in Figure 7.

In acetonitrile solutions at 295 K, the MLCT E_{max} values for the ethynyl-containing complexes are always slightly higher than those of their ethenyl analogues. With the exception of **13** and **23**, the same applies in butyronitrile glasses at 77 K, and the blue shifts are generally larger than those observed at room temperature. Blue shifting of ICT bands is also observed when comparing (*E*)-stilbenes with diphenylacetylenes, although the differences are considerably larger than those found here.[7,29b] While both types of complexes show small increases in E_{max} as n increases from 1 to 2 at 295 K, this behavior only applies at 77 K to the

(35) Willetts, A.; Rice, J. E.; Burland, D. M.; Shelton, D. P. *J. Chem. Phys.* **1992**, *97*, 7590.
(36) Lambert, C.; Nöll, G. *J. Am. Chem. Soc.* **1999**, *121*, 8434.

Table 6. MLCT Absorption, Electrochemical, Stark Spectroscopic, and HRS Data for the Complex Salts **1**−**11**, **13**, and **16**−**23**

salt	n	E_{max},[a] eV	$E_{1/2}$[$Ru^{III/II}$],[b] V vs Ag−AgCl	E_{max},[c] eV	f_{os}[c]	μ_{12},[d] D	$\Delta\mu_{12}$,[e] D	$\Delta\mu_{ab}$,[f] D	c_b^2 [g]	H_{ab},[h] cm^{-1}	β_0[S],[i] $\times10^{-30}$ esu	β_{1064},[j] $\times10^{-30}$ esu	β_0[H],[k] $\times10^{-30}$ esu
16[l,m]	1	2.08	0.43	1.82	0.23	5.5	16.2	19.6	0.09	4100	175	828	142
2	1	2.12	0.50	1.91	0.25	5.9	19.6	22.9	0.07	4000	216	1136	169
17[n,o]	2	2.12	0.42	1.84	0.43	7.9	22.4	27.4	0.09	4300	482	2593	372
3	2	2.14	0.49	1.87	0.28	6.3	23.4	26.6	0.06	3600	308	884	117
18[l,m]	1	2.20	0.62	1.94	0.25	6.0	19.3	22.7	0.08	4100	218	904	78
5	1	2.22	0.65	2.01	0.24	5.6	19.8	22.7	0.06	4000	178	1077	78
19[o]	2	2.25	0.61	1.97	0.50	8.2	25.1	30.0	0.08	4300	514	1332	75
6	2	2.27	0.65	1.98	0.32	6.6	25.7	28.9	0.05	3600	331	1280	50
20[l,m]	1	2.05	0.44	1.80	0.26	6.3	18.0	22.0	0.09	4200	256	857	168
8	1	2.08	0.48	1.88	0.24	5.8	21.6	24.5	0.06	3600	241	1143	200
21[n,o]	2	2.09	0.41	1.81	0.48	8.4	23.3	28.7	0.09	4300	586	1440	237
9	2	2.12	0.46	1.86	0.34	7.0	27.6	31.0	0.05	3400	457	1300	193
22[p]	1	2.52	1.10	2.41	0.33	6.0	16.9	20.7	0.09	5600	123		
11[q]	1	2.54	1.15	2.44	0.38	6.4	18.2	22.3	0.09	5600	146	359	45
23[p]	2	2.53	1.09	2.45	0.94	10.0	20.6	28.7	0.14	6900	401		
13	2	2.57	1.14	2.45	0.22	4.9	22.8	24.8	0.04	3900	106	490	70

[a] Measured in acetonitrile solutions at 295 K. [b] Solutions of ca. 10^{-3} M in analyte and 0.1 M in $[NBu^n_4]PF_6$ at a Pt bead/disk working electrode with a scan rate of 200 mV s^{-1}. Ferrocene internal reference $E_{1/2} = 0.43$ V. [c] Measured in butyronitrile glasses at 77 K. [d] Calculated from eq 2. [e] Calculated from $f_{int}\Delta\mu_{12}$ using $f_{int} = 1.33$. [f] Calculated from eq 1. [g] Calculated from eq 3. [h] Calculated from eq 4. [i] Calculated from eq 5. [j] Obtained from 1064 nm HRS measurements in acetonitrile solutions at 295 K. [k] Derived from β_{1064} by application of the two-state model.[34] [l] Reference 23. [m] Reference 31. [n] Reference 4b. [o] Reference 4c. [p] Reference 11 (HRS not measured). [q] Data taken in part from ref 11.

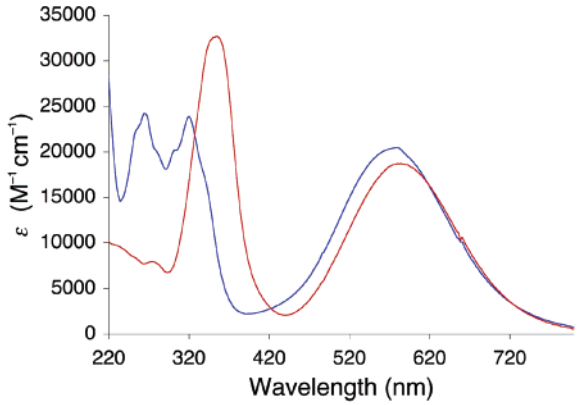

Figure 7. UV−visible absorption spectra of salts **3** (blue) and **17** (red) in acetonitrile at 295 K.

ethenyl-containing complexes, whereas the ethynyl species then show red shifts as the conjugation is extended (except for **11** and **13**). In all cases, the ethynyl-containing chromophores have slightly higher $Ru^{III/II}$ $E_{1/2}$ values (by 30−70 mV), showing that increasing the degree of unsaturation causes the Ru centers to become less electron-rich. This observation is attributable to the mildly electron-donating properties of ethenyl units.

The values of f_{os}, μ_{12}, c_b^2, and H_{ab} for the $n = 1$ complexes are generally similar, irrespective of the nature of the conjugated bridge, but in the $n = 2$ systems, all of these quantities are larger in the ethenyl-containing chromophores. These results are consistent with orbital overlap and consequent D−A electronic coupling being relatively unaffected by the nature of the π bridge in the short complexes but decreasing (or remaining relatively constant) upon extension in the ethynyl systems. This behavior is broadly consistent with studies on related purely organic molecules, and a relative insensitivity of the ICT band intensity and μ_{12} on n has been noted in diphenylpolyynes.[29] As expected, the values of $\Delta\mu_{12}$ and $\Delta\mu_{ab}$ increase with n (and therefore length) for both types of complexes and are generally not substantially affected upon moving between doubly and triply bonded linkages.

Although the relatively large estimated error (±20%) on the results renders comparisons difficult, the β_0[Stark] values generally decrease upon moving from an ethenyl- to ethynyl-containing complex, and this effect appears more consistent and significant in the $n = 2$ species. It is also worth noting that we were able to obtain Stark data for the low-energy ILCT bands of **17**, **19**, and **21**, giving respective total β_0[Stark] values of 546, 565, and 645 × 10^{-30} esu.[4c] Although their higher energies meant that we could not similarly analyze the ILCT transitions of **3**, **6**, and **9**, the contributions of these to the NLO responses will inevitably be less signficant than those in the cases of **17**, **19**, and **21**. Therefore, the decreases in the total β_0 upon replacing a (*E*,*E*)-buta-1,3-dienyl with a buta-1,3-diynyl linkage are likely to be larger than those indicated by the data shown in Table 6. The lack of HRS data for **22** and **23** means that the β_0[H] values can only be compared for the ammine complexes; these results do not present a consistent picture, but in the cases where a significant difference is observed (for the pairs **17**/**3** and **19**/**6**), β_0[H] is larger for the ethenyl-containing complexes.

Somewhat different dependencies of β_0 on n are observed for the ethenyl- and ethynyl-containing complexes. For the ethenyl chromophores, β_0[Stark] always increases sharply (by 2-fold or more) upon moving from $n = 1$ to 2, but the same structural change produces smaller increases in the ethynyl species, and moving from **11** to **13** even produces a decrease. The origin of this differing behavior can be traced primarily to larger increases in μ_{12} upon extending the conjugation in the ethenyl chromophores. Again, the observation of differing dependencies of the NLO response on the conjugation length for the two types of π systems is broadly in agreement with previous studies on related purely organic chromophores; whereas β_0 increases markedly with n in polyenes,[6,7] moving from $n = 1$ to 2 in the corresponding

polyynes causes smaller (or even insignificant) changes in the NLO response.[6,7,29b,c]

Conclusions

We have synthesized and characterized a number of new ruthenium(II) pyridyl complexes containing ethynyl or buta-1,3-diynyl linkages to pyridinium electron acceptor groups, with the primary aim of drawing comparisons with analogous ethenyl-containing chromophores. In acetonitrile solutions at 295 K, the new complexes display unusual blue shifting of MLCT bands as the conjugation is extended, which resembles the behavior of the corresponding ethenyl systems. Both the MLCT energies and electrochemical data confirm the superior electron-donating ability of ruthenium(II) ammine centers when compared with a *trans*-$\{Ru^{II}Cl(pdma)_2\}^+$ unit. HRS measurements at 1064 nm and Stark spectroscopic studies have been used to provide direct and indirect estimates of β_0 responses, and it is found that both the linear and NLO properties show temperature and medium dependence. Thus, at 77 K in butyronitrile glasses, the MLCT bands display a more normal red shifting with increased conjugation length. While the Stark-derived β_0 values generally increase as n (the number of ethynyl units) increases from 0 to 2, the HRS data show maximization at $n = 1$ for two of the ammine series but an increase upon moving from $n = 1$ to 2 for the pdma complexes. Comparisons with the analogous ethenyl chromophores show that the latter generally display larger β_0 values, whether determined via HRS or Stark data, and the inferiority of the ethynyl systems in terms of NLO response is more pronounced for the longer molecules where $n = 2$. The origin of this differing behavior is attributable primarily to larger increases in μ_{12} (which is related to D−A π-electronic coupling) upon extending the conjugation in the ethenyl chromophores, with changes in the MLCT energy and $\Delta\mu_{12}$ being less significant factors. The observation of generally larger β_0 values, which increase more with elongation, in ethenyl as opposed to ethynyl species is consistent with previous studies on related purely organic D−A chromophores.

Acknowledgment. We thank the EPSRC for support (a Ph.D. studentship) and also the Fund for Scientific Research-Flanders (FWO-V, G.0297.04), the University of Leuven (GOA/2006/3), and the Belgian Government (IUAP P5/3). We are also grateful to Dr. Lathe A. Jones for some preliminary synthetic studies.

Supporting Information Available: X-ray crystallographic data in CIF format. This material is available free of charge via the Internet at http://pubs.acs.org.

IC051816+